

Synthesis and characterization of Tin oxide thin film, effect of annealing on multilayer film

Mohamed Shaban^{1*}, G. F. Attia², Mohamed A. Basyooni², Hany Hamdy¹

¹ Nanophotonics and Applications (NPA) Lab, Department of Physics, Beni-Suef University, Beni-Suef 62111, Egypt

² Space Research Lab, Solar and Space Research Department, National Research Institute of Astronomy and Geophysics (NRIAG), Helwan, Cairo, Egypt.

Abstract- Nano crystalline Tin oxide thin film of multiple layers was successfully prepared by the sol-gel method with, spin coater has been used to deposit the films. The starting material is SnCl₂. The SnO₂ material was characterized by X-ray Diffraction (XRD), Scanning Electron Microscope (SEM). The optical properties (A, T, R) of the SnO₂ thin film of various annealing temperatures (400,500,600 Co) have been studied. Characterization results indicated that the products are composed of crystalline SnO₂ nanoparticles which exhibit the cassiterite-type tetragonal crystal structure. SEM revealed that with increase annealing temperature, the uniformity of the film increased. XRD measurements showed that the grain size increased from 1.06, 1.48, 1.71 nm. The variations of the refractive index (n), extinction coefficient (K) and Optical Conductivity with the wavelength have been studied. Nevertheless, the variation of the optical band gap with film thicknesses shows a significantly decrease in the values of the band gap with increase the film thicknesses.

* **Correspondence Author** – Tel.: +20-111-212-4309; +20-127-449-3440; Fax: +2-082-233-4551; Email: mssfadel@yahoo.com.

Keywords- SnO₂ thin film, XRD, Spin coater, annealing temperatures, Sol-gel.

1. INTRODUCTION

SnO₂ film is a wide band gap (3.6eV) n-type semiconductor with a highly resistant to moisture and acids [1], gas sensing materials for gas sensor devices [2], aerospace vehicles [3]. The methods that have been employed to prepare SnO₂ thin films include photochemical deposition [4], RF sputtering [5], sol-gel process [6, 7] chemical vapor deposition [8, 9], physical vapor deposition [10], spin-coating [11] and spray pyrolysis [12]. Sol-gel technology has emerged as an ideal fabrication method due to its low processing cost and its ability to control the morphology of the film. It has been reported that SnO₂ films prepared by spin-coating method can be used as gas sensors [13–15] and solar cell system electrode materials.

2. EXPERIMENTAL DETAILS

SnCl₂·2H₂O was used as precursor material. 8.374 gm of SnCl₂·2H₂O was dissolved in 100 ml of absolute ethanol. The mixture was refluxed and stirred at 353 K for 3 hours and then it was allowed to cool to the room temperature for 1 hour with continuous stirring. We used a glass substrate to deposit the solution with the help of the commercial spin coater Figure (1). For film deposition, the glass substrates were cleaned for 30 minutes in H₂SO₄ : H₂O₂ : 3 : 1, then for 10 minutes in acetone with boiling temperature, also for 10 minutes in methanol with boiling, then rinsed in de-ionized water and dried in 150C. We kept the spin coater speed at 2100 rpm for 30 seconds. We started from one layer until twelve ones and under those conditions, we found that the twelfth one was the fitted one. With twelve multi layers, the coated glass slide was air annealed at 400, 500 and 600 for 10 minutes. The slide was then allowed to cool to the room temperature.

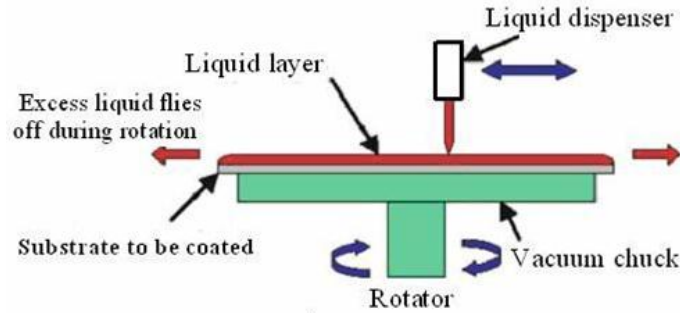


Fig. 1: Schematic of spin coating process.

3. RESULTS AND DISCUSSION

3.1. SEM studies

Figure 2. (a, b, c) show the SEM images for the SnO₂ thin films calcinated at 400, 500, 600 °C, respectively. Obviously, that the uniformity increases with increase the annealing temperatures.

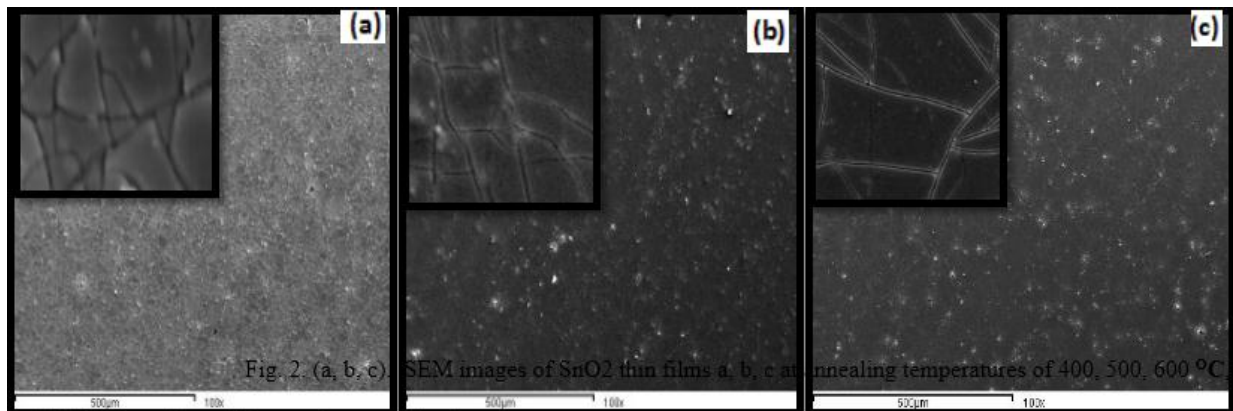


Fig. 2. (a, b, c). SEM images of SnO₂ thin films a, b, c at annealing temperatures of 400, 500, 600 °C, respectively.

3.2. EDS analysis (Chemical composition):

Fig. (3). Shows the EDS spectrum of SnO₂ thin film annealed at 400,500,600 °C.

In the samples the oxygen element component (atomic %) are observed to be almost twice that of tin, hence confirming the chemical composition to be SnO₂.

No other impurities are detected confirming high purity of the SnO₂ thin film.

Element	Weight%	Atomic%
OK	36.47	80.99
SnL	63.53	19.01
Totals	100.00	

Element	Weight%	Atomic%
OK	25.17	71.39
SnL	74.83	28.61
Totals	100.00	

Element	Weight%	Atomic%
OK	24.96	71.16
SnL	75.04	28.84
Totals	100.00	

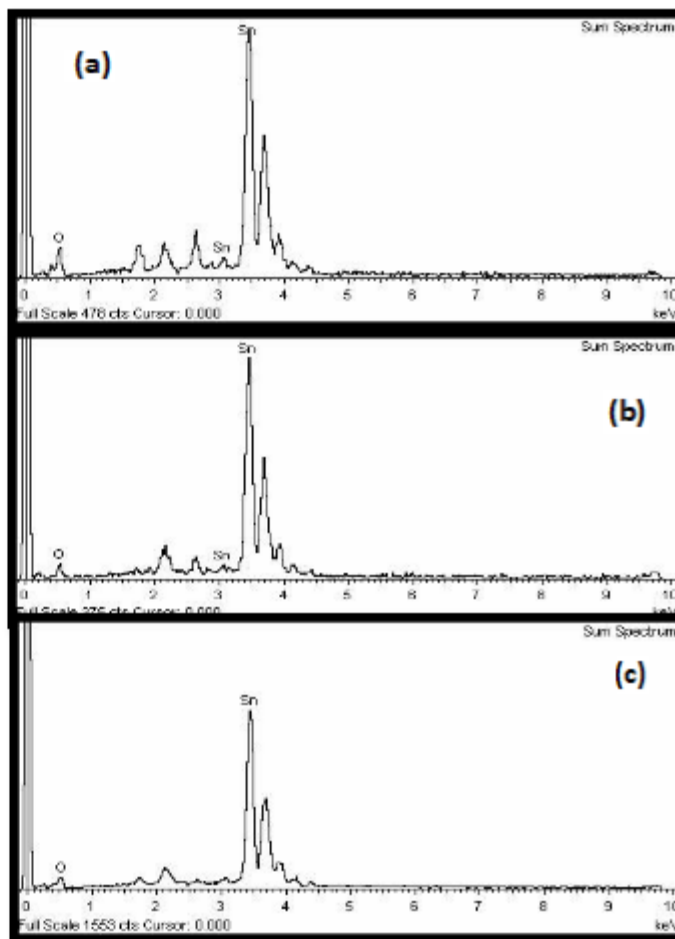


Fig.3. (a ,b, c) the EDX results of the as prepared SnO₂ thin films which annealed at 400, 500, 600 C°, respectively.

3.3 XRD results

Structural analysis of the deposited SnO₂ film was carried out by using CuK α radiation source having wavelength 1.5406 Å. The X-ray diffraction pattern of the film is recorded. Reflections from the tetragonal crystallographic phase (cassiterite) of SnO₂ that match standard inter planar spacing JCPDS card no. 01-077-0452 became sharp with increase the annealing temperatures.

From Figure 4. (a), we estimated that the spin coater time run cycle was affected the deposited films. We tested the deposited films under a constant spin coater's speed (2100 rpm), a number of layers (12-layers), and the annealing conditions (400 °C, and 10 min) and we changed only the spin coater's run cycle time as 15, 30 seconds. We found a difference in the XRD intensity. In the case of "30 seconds", the XRD intensity is higher than that of "15 seconds". Dependently, in the next steps, we will keep our spin coater's time as 30 seconds.

Fig.4(b) shows the XRD for 12 and 24 multilayer thin films at 2100rpm and an annealing temperature of 400C°. In our work, we started to deposit a multi-layered thin films and measured the corresponding XRD results, we found that with increase the deposited films, the crystallization becomes more clear and intensive. And we found that the 12-layered deposited films with 2100rpm and the spin coater run cycle time is 30 seconds, are the best.

Fig.4(c) shows the XRD results of the 12-multi layered SnO₂ thin films with 2100rpm as the spin coater speed, 30 seconds as the spin coater run cycle time and different annealing temperatures (400,500,600C°) with a constant annealing time of 10 min for all cases. With increase the annealing temperatures, crystalline nature of the deposited SnO₂ films sets in. With increase the annealing temperatures the SnO₂ thin films became more defined and

progressively more intense and sharp. It is evident that the films show only SnO₂ peaks with its preferred orientation directions at (110), (101), (200), (211), (220), (002), (310), (112), (301), (202), and (321). Since all peaks are sharp for high temperatures, it is evident that the film is polycrystalline in nature. The grain size was calculated by XRD peaks, which has the maximum intensity. Using Sherrer's equation the grain size can be calculated as:

$$D = 0.94\lambda / \beta \cdot (\cos \theta),$$

Where D is the average grain size, $\lambda = 1.5406 \text{ \AA}$ is X-ray wavelength and β is the peak FWHM and θ is the diffraction peak position. On the other hand, the diffraction peaks in the XRD pattern are very sharp with the high intensity indicating the significant increase in grain size. The particles size are 10.6, 14.8, 17.1 nm corresponds to annealing temperatures 400,500,600 C°, respectively. The variation of annealing temperatures with the grain size is plotted in figure 4. (d), which shows that the grain size increased with increase the annealing temperature.

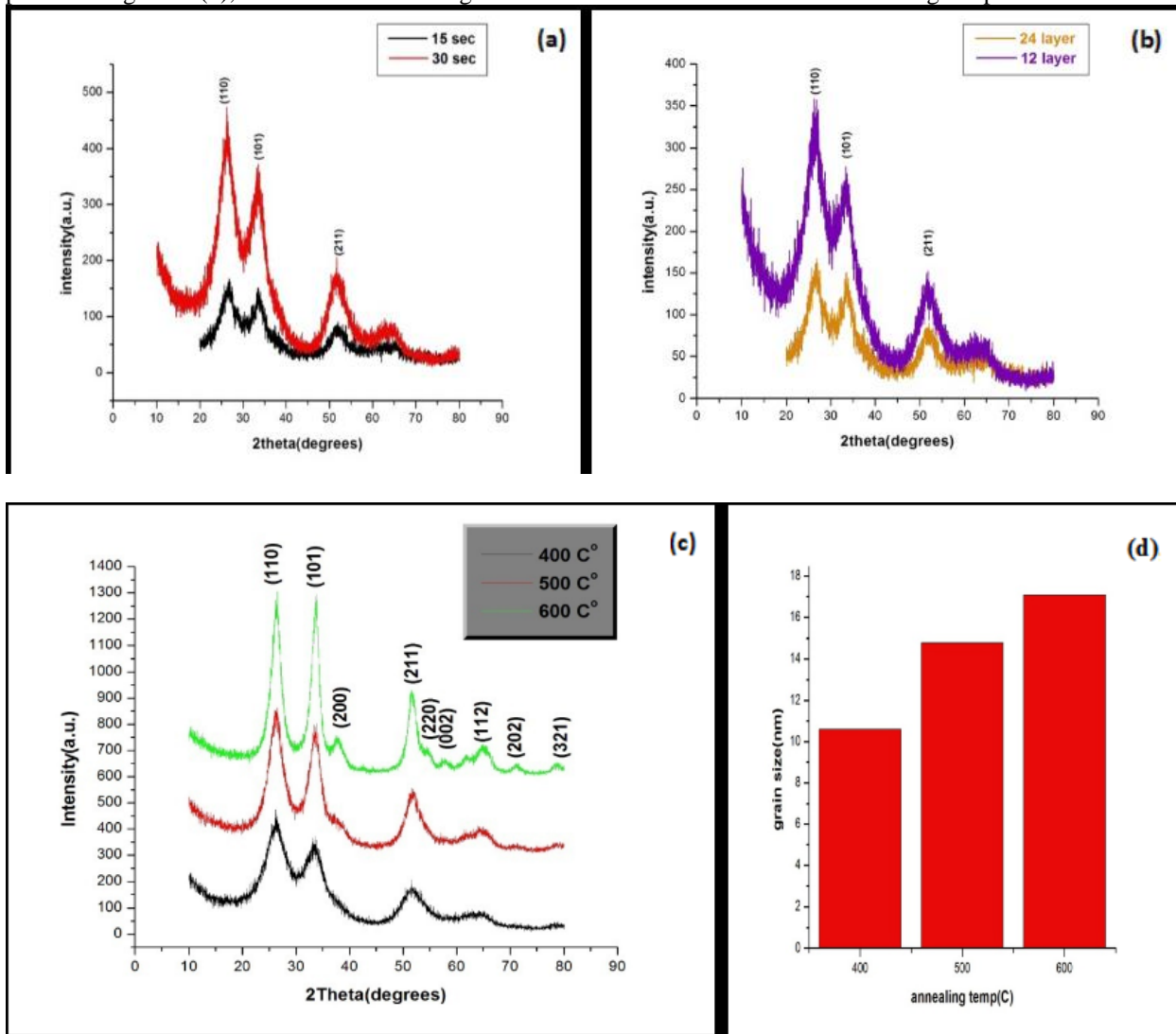


Figure.4.(a),represent the X-ray diffraction patterns of the SnO₂ thin films at 2100rpm and 15,30 seconds as the spin coater run cycle. Figure.4.(b), represent the XRD of the SnO₂ thin films at 2100rpm and 30 seconds as the spin coater run cycle with 12,24-deposited layers and 400 C° as the annealing temperature. Fig. 4(c), represent XRD of the SnO₂ thin films at 2100rpm and 30 seconds as the spin coater run cycle with varying the annealing temperatures, 400,500,600C°. Fig. 4(d) shows the variation of grain size with annealing temperature.

3.4. Optical studies:

3.4.1. Optical transmittance spectra

Fig.5(a), UV-Vis Spectroscopy has been used to investigate the optical transmission (T) of 12 and 24 multilayer SnO₂ films annealed at 400 °C which deposited on glass substrates. A sharp fall in transmission at about 310 nm is due to the absorption of the glass substrate. The transmission of films decreases with increase the deposited layers. This may be due to the increase in the film thickness which is also clear from the fringes in the transmission curves. From fig.5 (b) the transmission curves of the as prepared SnO₂ thin films of 12-layered which annealed at various temperatures (400,500,600 C°). It provide us, that with increase the annealing temperatures (film thicknesses), the transmission decreases.

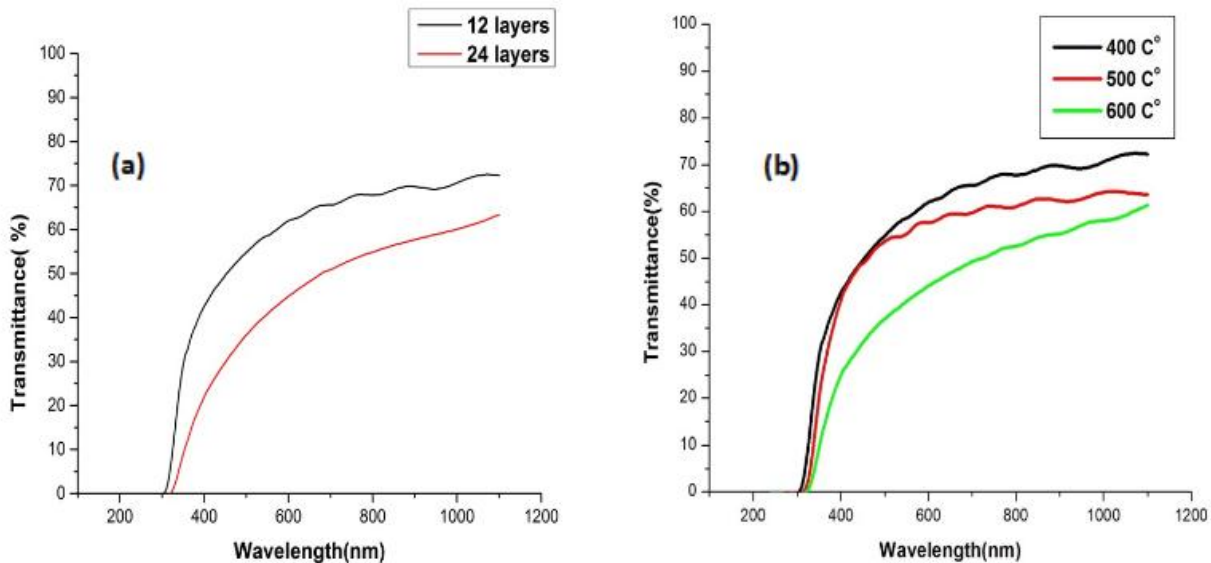


Fig.5(a) Optical transmission spectra- wavelength (nm) curve of 12 and 24 multilayered layered SnO₂ film annealed at 400 Co. Fig.5(b) shows the transmittance variation of 12 layers SnO₂ thin films annealed at 400,500,600C°

3.4.2. Theory of thickness measurement

The film thicknesses were calculated using the envelop method developed by Manificier et al.

Refractive index (n) of the thin film can be calculated as:

$$n = \{N + (N^2 - \mu^2)^{1/2}\}^{1/2}$$

Where;
$$N = 2\mu \frac{T_u - T_l}{T_u T_l} + \frac{\mu^2 + 1}{2}$$

And μ is the refractive index of the substrate (=1.53 for glass). T_u and T_l are the transmission maximum at upper envelops and transmission minimum at lower envelop for a particular wavelength λ .

$$d = \left| \frac{\lambda_1 \lambda_2}{4(n_1 \lambda_2 - n_2 \lambda_1)} \right|$$

We will mathematically calculate the thickness of the 12-layered thin film which annealed at 400 C and the same for 500,600C°

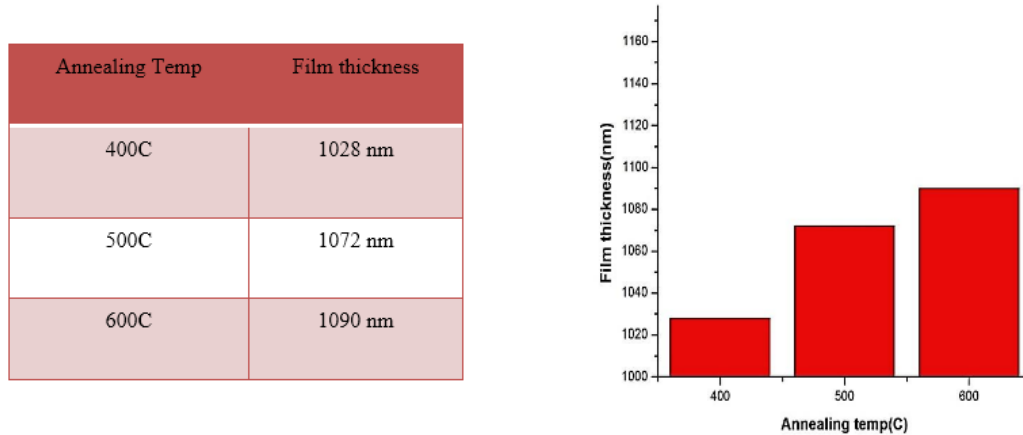


Fig. 6. Table (1) shows the variation of annealing temperature with film thickness.

We found that the film thicknesses increased with increase the annealing temperature as shown the table (1)

3.4.3. Absorption spectrum:

The absorption coefficient can be calculated from the Lambert's formula.

$$\alpha = (1/d) \log (1/T)$$

Where, d = is a thickness of the film, T= is a transmittance of the film.

Figure.7; show the absorption Spectrum of the 12-layered thin film which annealed at 400,500,600C° SnO₂.

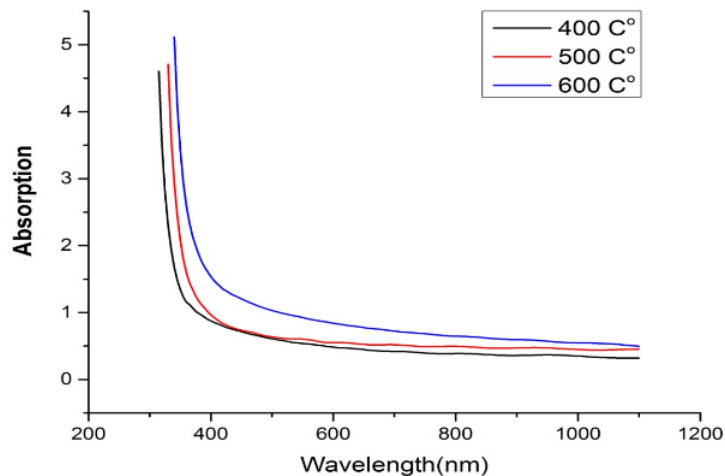


Fig.7. Absorption Spectrum of the 12-layered thin film which annealed at 400,500,600C° SnO₂

3.4.4. Optical Band Gap (E_g) Characterization

Fig. 8 shows the variation of $(\alpha hv)^2$ & (hv) for the determining the band gap E_g of SnO₂ films of various thicknesses by extrapolation of curve. The incident photon energy is related to the direct band gap E_g by equation:

$$(\alpha h\nu) \propto (h\nu - E_g)^{1/2}$$

From table (2), it is observed that the optical band gap blue-shifted with increase the annealing temperatures and the film thicknesses, as well. Generally, the effect of band gap variations with film thicknesses owing to:

- (i) Effect of quantum size
- (ii) Large density of dislocations
- (iii) Change in barrier height owing to change in grain size in polycrystalline films

Owing to the films thicknesses are large which may causes dislocations and defects during the films preparations can support the second reason.

Table 2. Variation of optical band gap with film thickness of SnO₂ films. It is clear that by increases the temperature, energy gap was decreased.

Annealing Temp (C°)	Film thickness(nm)	Optical band gap(eV)
400	1028.668543	3.7
500	1072.593407	3.6
600	1090.493067	3.5

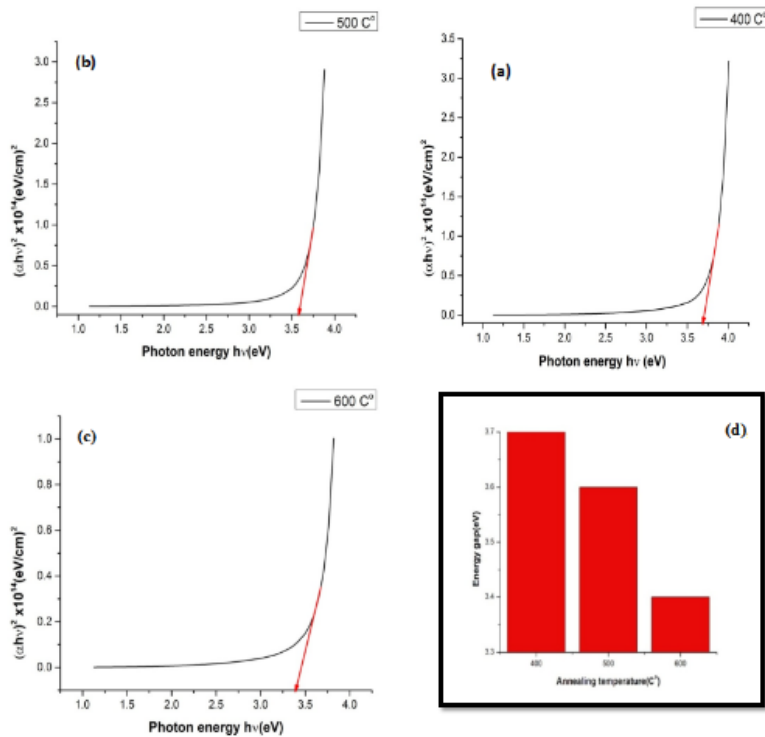


Fig. 8 (a,b,c). The plots of $(\alpha E)^2$ vs. photon energy E_g of SnO₂ thin film deposited with spin coating at 2100 rpm on glass substrate and annealed for 10 min at 400, 500, 600 C°. Fig. 8(d) represents the variation of energy gap with the annealing temperatures

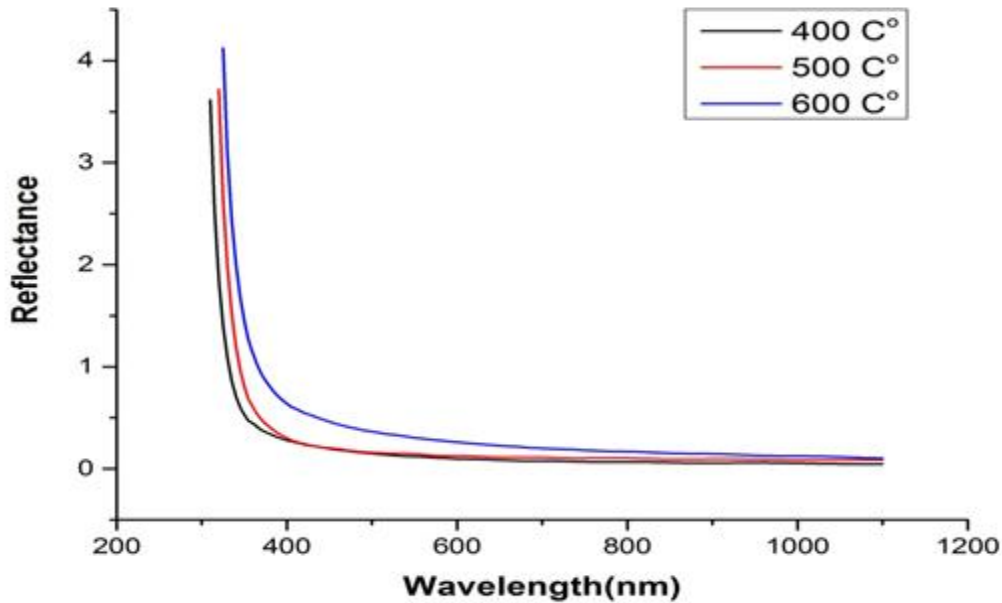


Fig. 9. Reflectance Spectra of SnO₂ thin film of 12 layers which annealed at 400 Co

3.4.5. Reflectance (R) spectrum:

The reflectance (R) has been found by using relationship:

$$R+T+A=1$$

3.5. Determination of the Optical Constants, Refractive Index, n and Extinction Coefficient, k:

The complex refractive index is defined by:

$$N(\omega) = n + iK$$

Where n is the refractive index and k is the extinction coefficient, n of a thin film can be determined by the following relation:

$$n = \left[\frac{1+R}{1-R} \right] + \sqrt{\frac{4R}{(1-R)^2} - K^2} ,$$

Where R is the reflectance. And the extinction coefficient of a thin film can be determined by the following relation:

$$K = \frac{\alpha\lambda}{4\pi}$$

Where α is the absorption coefficient of the film, and λ is the wavelength of light.

Fig.10 (a, b, c), shows the variation of refractive index and the extinction coefficient with wavelength. It can be seen that, the both factors decreased with the wavelength according to the behavior of reflectance spectrum.

The refractive index of SnO₂ as reported before, at 550 nm was 2.00 and the extinction coefficient was 0.03. In our work, the refractive index at $\lambda = 549.7163\text{nm}$ is 2.0 and the extinction of coefficient at $\lambda = 499.01$ is 0.0288

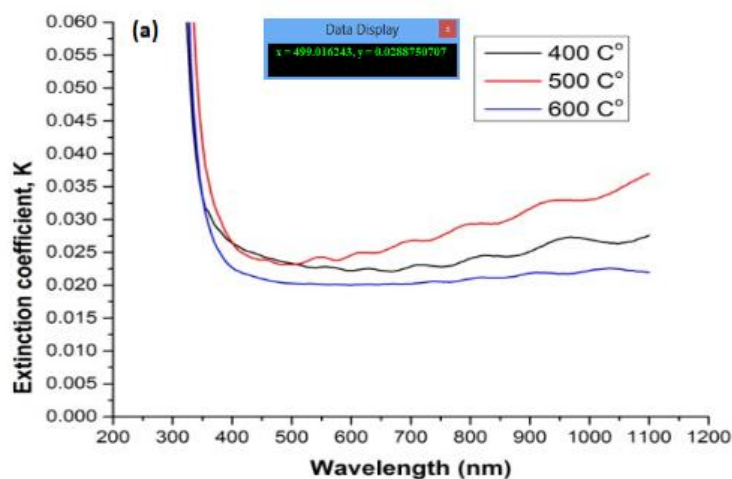


Fig.10 (a, b). The variation of extinction coefficient(K) and refractive index(n), respectively, of SnO₂ thin film of 12 layers which annealed at 400,500,600 C°

4. CONCLUSION

We studied the effect of annealing temperature on a multilayer spin coated tin oxide thin films by sol-gel technique. It was found that the surface morphology changes with the different annealing temperatures. The transmittance and the optical band gap decrease with increase the film thickness while the refractive index increases.

REFERENCES

- [1] Igwe H U and Ugwu E I 2010 Optical characteristics of nanocrystalline thermal annealed tin oxide (SO₂) *Adv. Appl. Sci. Res.* **1** 240–6
- [2] Patil G, Kajale D D, Chaven D N, Pawar N K, Ahire P T, Shinde S D, Gaikwad V B and Jain G H 2011 Synthesis, characterization and gas sensing performance of SnO₂ thin films prepared by spray pyrolysis. *Bull. Mater. Sci.* **34** 1–9
- [3] Hunter, G.W.;Liu, C.C.;Makel, D.D. In MEMs Handbook Design and Fabrication ; 2ed.;CRC Press LLC:Boca Raton, FL, 2006, Chapter **11**.
- [4] Daisuker I and Masaya I 2006 Room temperature hydrogen sensing properties of SnO₂ thin films fabricated by the photochemical deposition and doping methods *Jpn. J. Appl. Phys.* **45** 7094–6
- [5] Kim D H, Lee S H and Kim K 2001 Comparison of CO-gas sensing characteristics between mono- and multilayer Pt/SnO₂ thin films. *Sensors Actuators B* **77** 427–31
- [6] Park S and Mackenzie J D 1995 Sol-gel-derived tin oxide thin films. *Thin Solid Films* **258** 268–73
- [7] Mishra S, Ghanshyam C, Ram N, Shing S, Bajpai R P and Bedi R K 2002 Alcohol sensing of tin oxide thin film prepared by sol–gel process. *Bull. Mater. Sci.* **25** 231–4
- [8] Jeong J, Choi S P and Hong K J 2006 Structural and optical properties of SnO₂ thin films deposited by using CVD techniques. *J. Korean Phys. Soc.* **48** 960–3
- [9] Liu Y, Koep E and Liu M 2005 A highly sensitive and fast-responding SnO₂ sensor fabricated by combustion chemical vapor deposition. *Chem. Mater.* **17** 3997–4000
- [10] Sberveglieri G, Faglia G, Groppelli S, Nelli P and Taroni A 1992 A novel PVD technique for the preparation of SnO₂ thin films as C₂H₅OH sensors. *Sensors Actuators B* **7** 721–6
- [11] Gu F, Wang S F, Lü M K, Cheng X F, Liu S W, Zhou G J, Xu D and Yuan D R 2004 Luminescence of SnO₂ thin films prepared by spin-coating method *J. Cryst. Growth* **262** 182–5

- [12] Gordillo G, Moreno L C, de la Cruz W and Teheran P 1994 Preparation and characterization of SnO₂ thin films deposited by spray pyrolysis from SnCl₂ and SnCl₄ precursors. *Thin Solid Films* **252** 61–6
- [13] Sakai G, Baik N S, Miura N and Yamazoe N 2001 Gas sensing properties of tin oxide thin films fabricated from hydrothermally treated nanoparticles: dependence of CO and H₂ response on film thickness. *Sensors Actuators B* **77** 116–21
- [14] Vuong D D, Sakai G, Shimano K and Yamazoe N 2004 Preparation of grain size-controlled tin oxide sols by hydrothermal treatment for thin film sensor application. *Sensors Actuators B* **103** 386–91
- [15] Ray S, Gupta P S and Singh G 2010 Electrical and optical properties of sol-gel prepared Pd-doped SnO₂ thin films: effect of multiple layers and its as room temperature methane gas sensor. *J. Ovonic Res.* **6** 63–74